Progress In Electromagnetics Research, Vol. 145, 19–29, 2014

Miniaturization of Antenna for Wireless Application with Difference Metamaterial Structures

Maryam Rahimi[1], Ferdows B. Zarrabi[2, *], Rahele Ahmadian[1], Zahra Mansouri[3], and Asghar Keshtkar[1]

Abstract—In this paper, periodic structures are investigated in antenna design for wireless applications. These antennas were compared with CRLH miniaturization method. Three different models of patch antenna with coaxial feed on EBG ground, metamaterial substrate or EBG/AMC structure have been presented here. Also two compact dual-band antennas have been designed and fabricated based on CRLH techniques for wireless and GSM applications. The first antenna has directional pattern and operates at 1760, 2550 and 3850 MHz (three-band antenna) with gain 2.1, −3.9 and 2.5 dBi, and it is dual polarized. The size of prototype patch antenna is $20 \times 20\,\text{mm}^2$ which is reduced about 47% in comparison to conventional patch antenna at 2.5 GHz. The second antenna is designed by the use of interdigital capacitor and spiral inductor. Dimensions of antenna are $15.5 \times 12\,\text{mm}^2$, so the size is reduced about 69% in comparison to conventional microstrip patch antennas at 1.8 GHz. The second tri-band antenna operates at 1060 MHz, 1800 MHz and 2500 MHz in which two frequencies (1.8 and 2.5 GHz) are suitable for GMS and WLAN applications. Both structures have been designed and fabricated on FR4 low cost substrate with $\varepsilon_r = 4.4$ and thickness of 1.6 mm. All simulations are done with CST and HFSS. Equivalent circuit and experimental results are also presented and compared.

1. INTRODUCTION

In recent decades, different types of wireless systems are widely used because of simplicity, low cost, high-speed data transfer and easy operation. Recently, with development of wireless devices such as mobile phones, portable computers and smart phones, new protocols are needed. IEEE 802.11a, IEEE 802.11bg and HyperLAN/2 standards cover WLAN frequencies. The IEEE 802.11 standard has three frequency bands at 2.4 GHz (2.484–2.4), 5.2 GHz (5.35–5.15) and 5.8 GHz (5.825–5.725), and the frequency range 3.3–3.8 GHz has been allocated to wireless personal area network (WPAN) and WiMAX [1–3].

Nowadays modern communication systems require microwave components with high performance and small size, so compact antennas are required. Microstrip antennas are used in aviation, space exploration, satellite, missile and various government and commercial applications, because of suitable size, weight, price, performance and ease of installation [4–7].

There is a need to design small size, easily fed and low cost antenna for multi-band applications. Slot antenna is a known antenna for wireless applications, with all attributes that WLAN communication systems need. Methods such as notch technique, metamaterial, slot and fractal methods are used in order to design multi-band antennas [8–10].

Composite right/left handed transmission line (CRLH-TL) technique is based on the use of artificial electromagnetic materials (metamaterial). These materials are periodic structures that are not found in nature and have been considered because of special characteristics and great variety of applications. In metamaterials, the real part of ε, μ or both of them are negative [11–14]. Metamaterials are widely

Received 9 December 2013, Accepted 23 January 2014, Scheduled 16 February 2014

* Corresponding author: Ferdows B. Zarrabi (ows.zarrabi@yahoo.com).

[1] Department of Electrical Engineering, Imam Khomeini International University, Qazvin, Iran. [2] Faculty of Electrical and Computer Engineering, University of Tabriz, Tabriz, Iran. [3] Department of Electrical Engineering, Sciences and Research Branch, Islamic Azad University, Tehran, Iran.

used in antenna and microwave circuits, in order to increase the miniaturization factor of the antenna, such as metamaterial structure in substrate [12], metamaterial load for miniaturization [13].

Electromagnetic band-gap structures (EBG) can be used for miniaturization and designing high gain patch antenna. Frequency selective structures (FSS) are defined as a periodic array of holes on a patch indicated on a substrate [15, 16]. These artificial magnetic materials have been used in substrate to increase effective permeability, thus the size of antenna will be reduced [17].

2. HOMOGENEOUS CRLH-TL THEORY

Metamaterial transmission line (MTL) is a type of TL structure which contains unit cells with series capacitor and shunt inductor. These elements are added to conventional transmission line model [18]. These new elements provide left handed (LH) propagation and support backward waves. Gap and interdigital capacitors are used as series capacitor but actually interdigital capacitors have higher capacitance. Vias are used as shunt inductors, but this inductance can be increased by combination with other types of inductors such as spiral or meander structures [19, 20]. We can also use spiral or meander structures as shunt inductor by adding virtual ground to them [20]. Zeroth-order resonators (ZOR) have become important structures for designing small antennas. They have much smaller size than traditional microstrip rectangular patch antennas. CRLH is a structure with both of the RH and LH characteristics [21, 22].

Equivalent circuit for a CRLH transmission line is shown in Figure 1. To achieve a structure with completely left-handed features is nearly impossible. According to the transmission line theory, propagation constant in lossless structure is $\gamma = j\beta = \sqrt{Z'Y'}$ where Z' and Y' are per unit length impendence and admittance [23].

MTL effective permeability and permittivity can be achieved by calculating Z' and Y' as presented in (1) [23]:

$$\mu = \mu(\omega) = L_R - \frac{1}{\omega^2 C_L} = \frac{Z'}{j\omega} \qquad \varepsilon = \varepsilon(\omega) = C_R - \frac{1}{\omega^2 L_L} = \frac{Y'}{j\omega} \tag{1}$$

where $Z' = j(\omega L_R - \frac{1}{\omega C_L})\,\Omega/\text{m}$, $Y' = j(\omega C_R - \frac{1}{\omega L_L})\,\text{S/m}$. $\omega_L = \frac{1}{\sqrt{C_L L_L}}$, $\omega_R = \frac{1}{\sqrt{C_R L_R}}$, $\omega_{se} = \frac{1}{\sqrt{C_L L_R}}$ and $\omega_{sh} = \frac{1}{\sqrt{C_R L_L}}$ are left-handed, right-handed, series and shunt resonance frequencies.

There is a frequency that separates the left-handed region from the right-handed one. We call it the transmission frequency, and it is calculate by the following equation [23]:

$$\omega_0 = \sqrt{\omega_R \omega_L} = \frac{1}{\sqrt[4]{L_R C_R L_L C_L}} \tag{2}$$

The input impedance of open ended boundary condition is obtained by (3) [23]:

$$Z_{in}^{open} = -jZ_0 \cot(\beta l) \overset{\beta \to 0}{\approx} -jZ_0 \frac{1}{\beta l} \qquad Z_{in}^{open} = -j\sqrt{\frac{Z}{Y}}\left(\frac{1}{-j\sqrt{ZY}}\right)\frac{1}{l} = \frac{1}{YNd} = \frac{1}{NY} \tag{3}$$

Propagation constant of CRLH-TL is determined by applying the periodic boundary conditions related to Bloch and Floquet theory. The CRLH TL unit cell's dispersion is obtained by:

$$\beta d = \cos^{-1}\left(1 - \frac{1}{2}\left(\frac{\omega_L^2}{\omega^2} + \frac{\omega^2}{\omega_R^2} - \frac{\omega_{sh}^2}{\omega_R^2} - \frac{\omega_{se}^2}{\omega_R^2}\right)\right) = \cos^{-1}\left(1 + \frac{1}{2}Z(\omega)Y(\omega)\right) \tag{4}$$

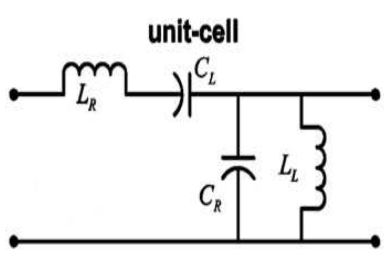

Figure 1. Equivalent circuit model of CRLH-TL unit cell.

3. ANTENNA STRUCTURE

In this article, different forms of patch antenna based on EBG, AMC and CRLH have been presented. All antennas are designed on FR-4 low-cost substrate with relative permittivity of 4.4 and loss tangent of 0.02. Antennas are fed by 50 Ω coaxial or microstrip line.

Figure 2 shows all designed and simulated antennas. Figures 2(a), (b) and (c) present patch antenna with EBG ground based on Fractal model, SRR rings and dumbbell SRR rings. Figure 2(d) indicates a patch antenna on metamaterial surface which is designed by SRR resonators. Figures 2(e), (f), (g), (h) and (i) show five different models of CRLH structure to miniaturize antenna for wireless applications. Interdigital structure and strip line are used for LH capacitance and inductance.

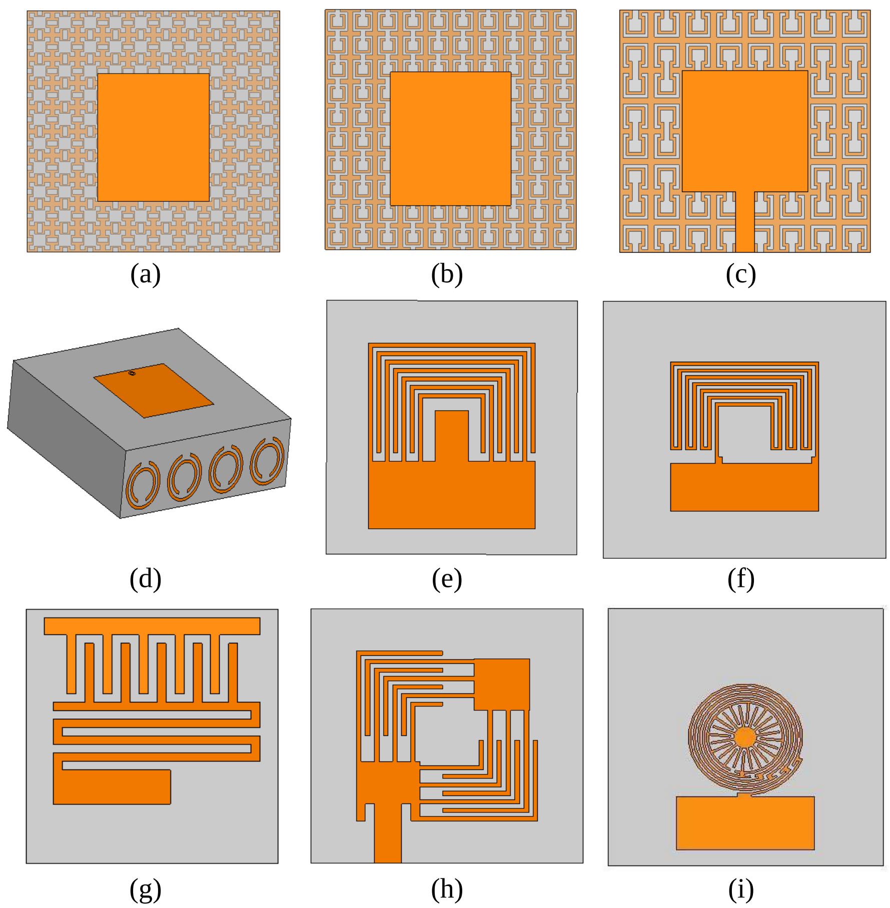

Figure 2. The geometry of patch antennas, (a) on fractal ground, (b) on SRR rings, (c) on dumbbell SRR rings, (d) SRR resonators, (e) Bent Interdigital capacitance, (f) with meandered load, (g) meandered Patch with Interdigital capacitance, (h) dual bent Interdigital, (i) Spiral CRLH structure.

4. SIMULATION RESULT

The antennas are simulated in HFSS. The return loss of antennas are shown in Figure 3. Figure 3(a) shows prototype antenna return loss with fractal EBG ground. This patch antenna with conventional ground plane has 80 MHz bandwidth. As shown here, the resonance frequency of antenna has been reduced around 200 MHz by the use of fractal EBG, so size reduction is achieved. Also in Figure 3(b) the return loss of the EBG SRR ground is presented. In this condition, the resonance has been changed less than 70 MHz. The return loss for patch antenna with dumbbell SRR rings is shown in Figure 3(c), and the antenna has 60 MHz bandwidth. The return loss for patch antenna with

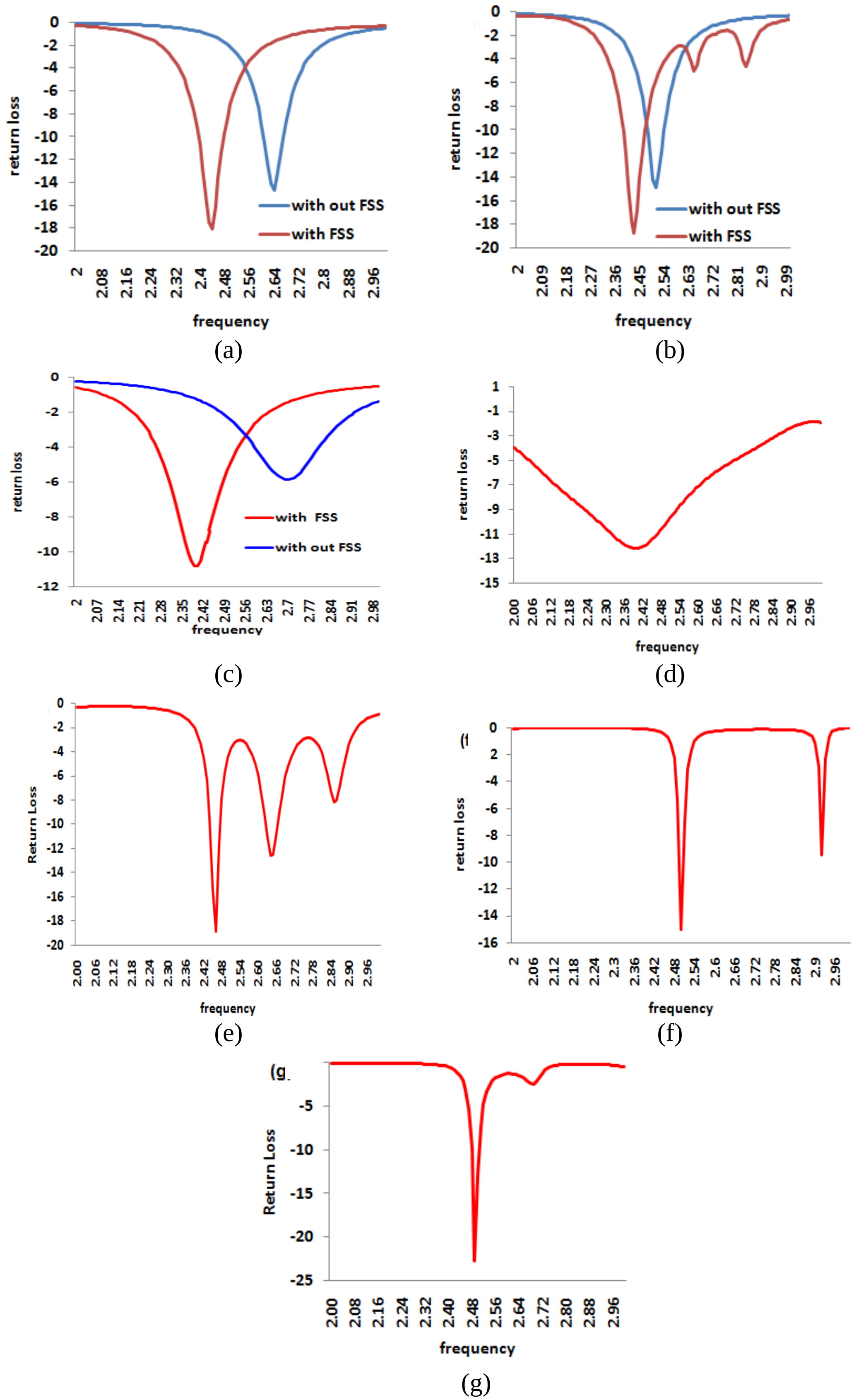

Figure 3. The return loss of difference model of patch antenna.

metamaterial substrate is shown in Figure 3(d), and this antenna has more than 270 MHz bandwidth for 2.4 GHz. Figure 3(e) shows the return loss of interdigital bent model with two resonance frequencies at 2.45 GHz and 2.65 GHz. Figure 3(f) shows the return loss of patch antenna with meandered load which resonances at 2.48 GHz with 25 MHz bandwidth. Figure 3(g) shows the return loss of meandered patch antenna with 35 MHz bandwidth at 2.45 GHz.

Figure 4 shows the gain of each antenna. Most of the antennas have a directional radiation pattern.

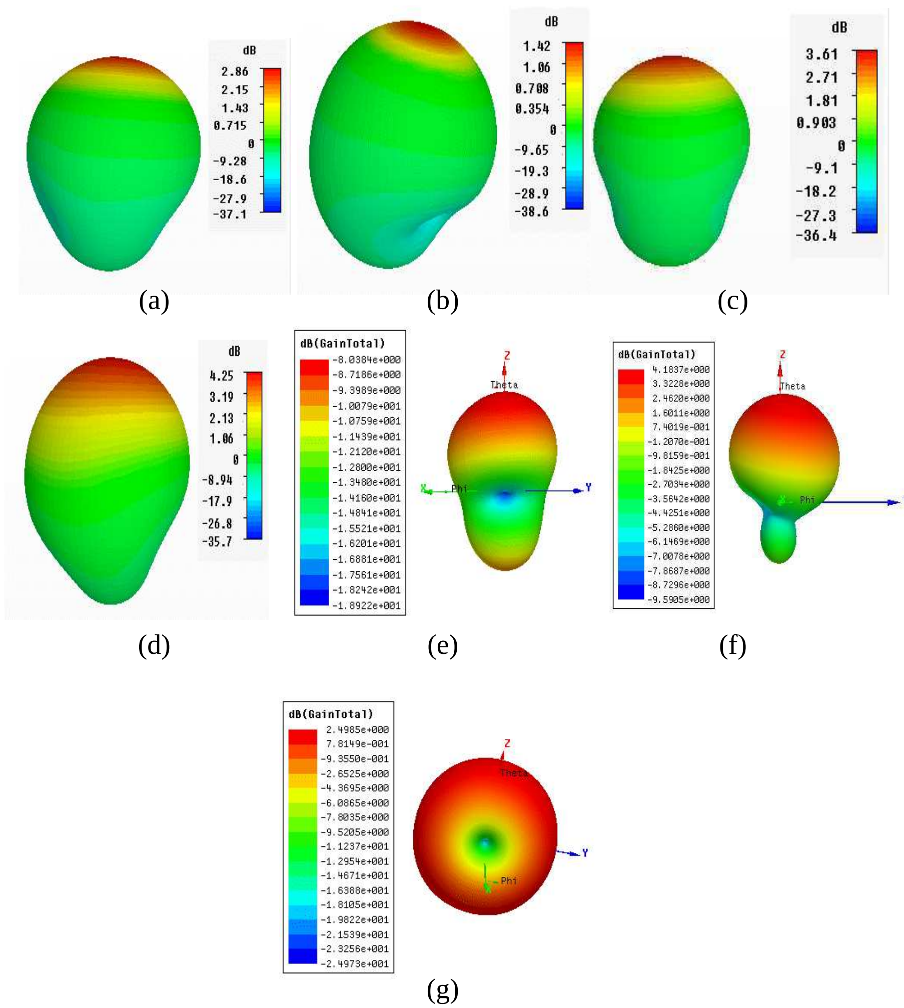

Figure 4. The pattern and gain for 2.45 GHz.

Table 1. comparison between presented models.

Antenna	Gain	BW	Patch Size	Total size
Fractal EBG	2.86 dBi	80 MHz	26.5 × 22	50 × 50 × 1.6
SRR EBG	1.42 dBi	80 MHz	27.8 × 24	50 × 50 × 1.6
SRR slot	3.61	25 MHz	25 × 24	40 × 40 × 1.6
Metamaterial Substrate	4.25 dBi	270 MHz	18 × 17	40 × 40 × 11.6
Interdigital Bent	−8.03 dBi	35 MHz	20 × 22	30 × 30 × 1.6
Patch with meandered	4.18 dBi	25 MHz	22 × 20	30 × 30 × 1.6
Meandered Patch	2.49 dBi	35 MHz	22 × 24	30 × 28 × 1.6

Figures 4(a), (b) and (c) show the patterns and maximum gains of EBG ground structures. The gain of the antennas are 2.86, 1.42 and 3.61 dBi. Figure 4(d) presents the SRR resonators pattern and gain. In this condition the antenna gain is around 4.25 dBi. Figure 4(e), (f) and (g) show the patterns and maximum gains of CRLH structures. The gains of the antennas are −8.03, 4.18 and 2.49 dBi.

In Table 1, the comparison of gain, bandwidth and size among the presented antennas is shown.

5. FABRICATION

The last two antenna models are fabricated. Figure 5 shows the prototype of the designed ZOR antenna. The first fabricated antenna model contains two parallel Interdigital capacitors, so it helps to increase the series capacitance, reduces the zeroth order resonator size and achieves more miniaturization factor. In fact, interdigital capacitor with L-shape fingers is presented which increases the capacitance value.

The rectangular patch antenna is fed by inset microstrip line with 7 mm length and 3 mm width which is connected to the 50 Ω SMA connector. Two parallel interdigital capacitors have connected this part to the other rectangular patch. The antenna is fabricated on FR-4 low-cost substrate with a dielectric constant of $\varepsilon_r = 4.4$ and thickness of 1.6 mm. The total size of the substrate is $30 \times 30\,\mathrm{mm}^2$, and patch total size is around $20 \times 20\,\mathrm{mm}^2$, so the miniaturization factor is 1.9.

The second antenna is proposed by the use of interdigital capacitor and a spiral inductor which is fed by a coaxial line. The second antenna is designed on a FR-4 low-cost substrate with dielectric constant 4.4 and loss tangent 0.02. The antenna is connected to coaxial 50 Ω feed line. The thickness of the substrate is 1.6 mm. Dimensions of the antenna are $15.5 \times 12\,\mathrm{mm}^2$, so the size is reduced about 69% in comparison to conventional patch antennas which resonates at 1.8 GHz. The antenna geometry

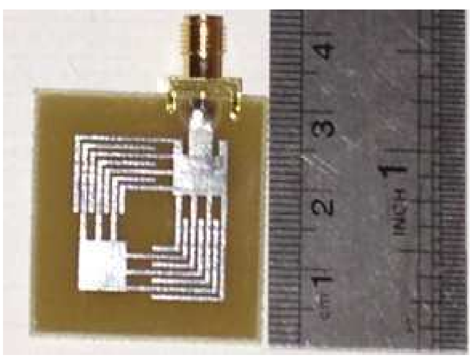

Figure 5. Geometrical model of the first fabricated antenna.

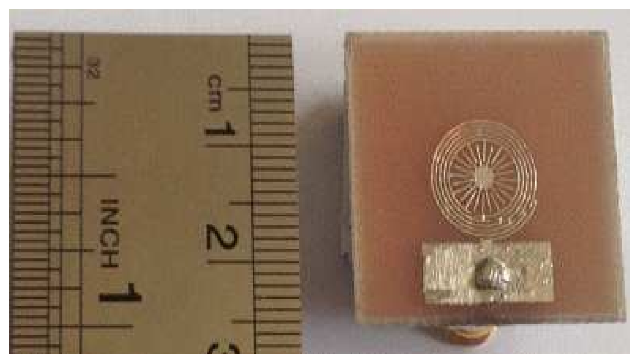

Figure 6. Second fabricated antenna geometry.

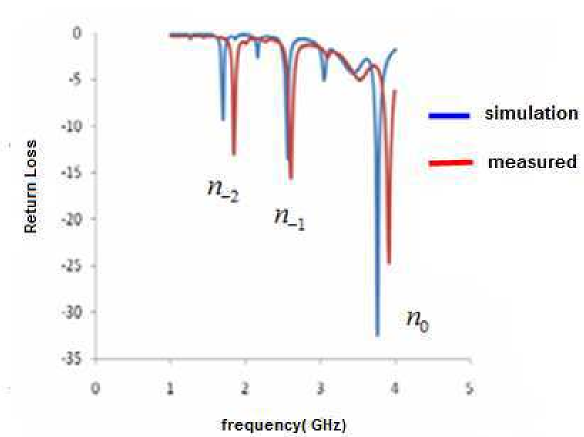

Figure 7. Return loss of the first antenna.

is shown in Figure 6. As shows in Figure 6, an interdigital capacitor is used here in circular form that is a new initiative. Circular interdigital capacitor is connected to spiral inductor and is fed through rectangular patch.

6. EXPERIMENTAL RESULT

The measured and simulated return losses of the first antenna are presented in Figure 7. The first model of the antenna has three bands with around 25 MHz, 32 MHz and 100 MHz bandwidth, respectively, at

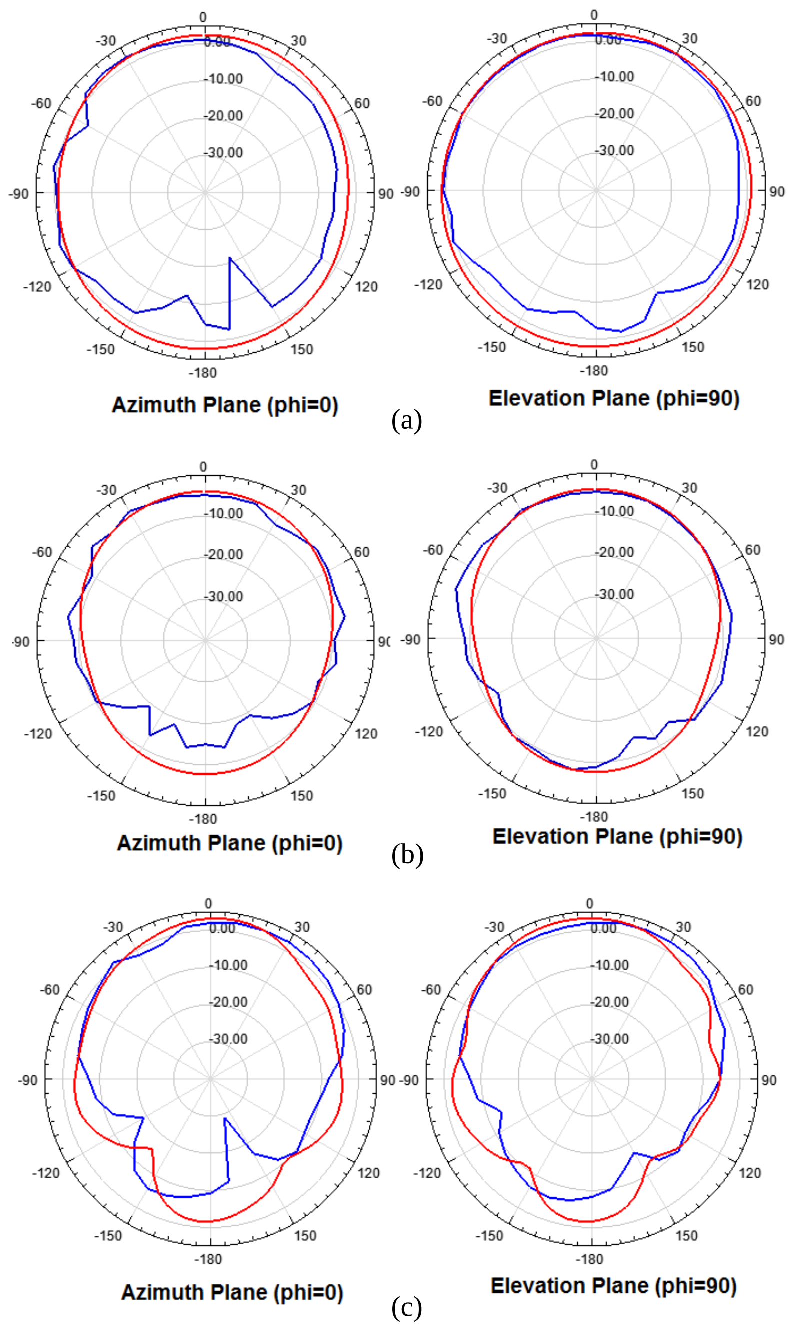

Figure 8. Pattern and gain of prototype antenna for azimuth plan, (a) 1.76 GHz, (b) 2.55 GHz, (c) 3.85 GHZ (blue for experimental, red for simulation).

1.76 GHz, 2.55 GHz and 3.85 GHz. The equivalent circuit parameters which are extracted from full-wave simulation data of the unit cell are $C_R = 0.69\,\text{pF}$, $L_R = 4.8\,\text{nH}$, $C_L = 0.32\,\text{pF}$ and $L_L = 2.5\,\text{nH}$. Therefore, $f_{sh} = 3.88\,\text{GHz}$ and $f_{se} = 4.08\,\text{GHz}$ so $f_0 = 3.9\,\text{GHz}$.

Figure 8 shows the measured radiation pattern of the first antenna in azimuth and evaluation plane for all frequencies. Also the maximum gains of the antenna at 1.76, 2.55 and 3.85 GHz are respectively 2.11, −3.9 and 2.5 dBi, as shown in Figure 8.

The first antenna shows circular polarization at 2.6 GHz. The measured axial ratio result is presented in Figure 9. For the calculation of axial ratio in chamber room, the antenna's horizontal and vertical fields have been tested at resonance frequencies. The first antenna is dual polarized, at 1.75 GHz and 3.85 GHz, which shows linear polarization, and at 2.55 GHz it has circular polarization.

The simulated efficiency is around 85%, 45% and 48% for 1760 MHz, 2500 MHz and 3850 MHz.

Traditional rectangular patch antenna printed on a FR4 substrate with 1.6 mm thickness and dimensions $29 \times 38\,\text{mm}^2$ will resonate at 2.4 GHz. Bandwidth of the traditional antenna is 80 MHz, and it has linear polarization. The dimensions of the presented antenna are $20 \times 20\,\text{mm}^2$, and it operates at three frequency bands (1.76 GHz, 2.55 GHz and 3.85 GHz) with respectively 25 MHz, 32 MHz and 100 MHz bandwidth. Also it shows circular polarization at 2.6 GHz because the current flows in a loop.

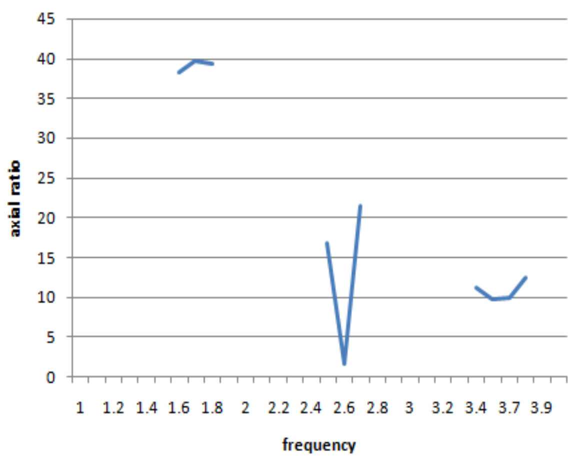

Figure 9. Measured axial ratio of presented antenna.

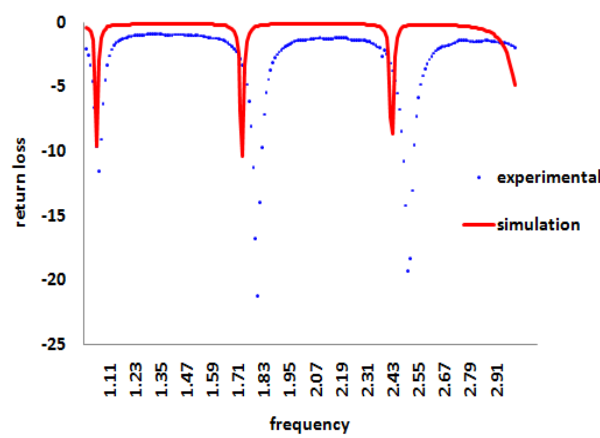

Figure 10. Comparison between experimental and simulated result.

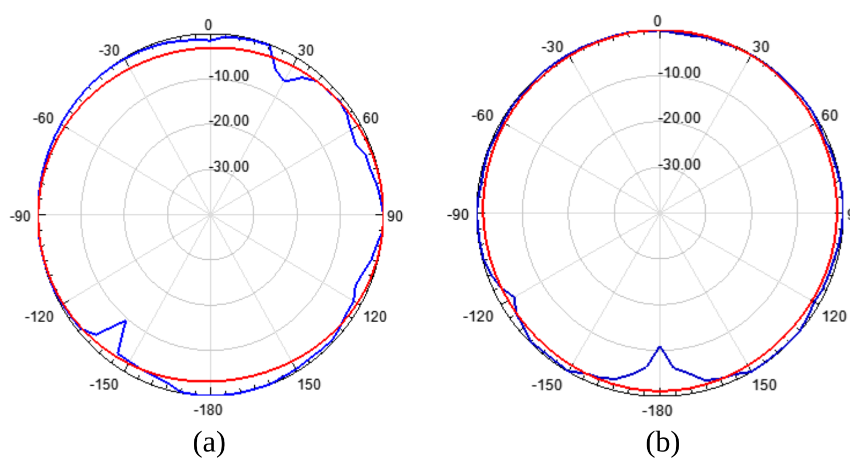

Figure 11. Azimuth pattern comparison in HFSS and experimental at (a) 1.8 GHz, (b) 2.4 GHz (blue for experimental, red for simulation).

The measured and simulated return losses of the second antenna are presented in Figure 10. The second antenna is tri-band with 30, 50 and 60 MHz bandwidth at 1060, 1800 and 2500 MHz resonance frequencies. The experimental radiation patterns of the antenna for 1800 and 2500 MHz are shown in Figure 11. The antenna has low gain, so it is suitable for indoor and medical care applications. The maximum gain of antenna at 2.4 GHz is around −8 dBi. The final prototype antenna is linear polarized with omnidirectional pattern.

Tables 2, 3 and 4 show comparison of characteristics, such as gain, bandwidth, size and polarization, between fabricated antennas and other ZOR metamaterial antennas for each frequency.

Table 2. Comparison for 1760 MHz.

parameter	First antenna	Second antenna	Ref. [24]	Ref. [19]
frequency	1760 MHz	1760 MHz	1760 MHz	1850
Gain	2.11 dBi	−12 dBi	5.4 dBi	6.4 dBi
BW	25 MHz	50 MHz	35 MHz	27 MHz
Total Size (mm)	$30 \times 30 \times 1.6$	$24 \times 24 \times 1.6$	$40 \times 40 \times 4$	$23 \times 58 \times 1.5$
Polarization	linear	linear	linear	linear

Table 3. Comparison for 2550 MHz.

parameter	First antenna	Second antenna	Ref. [25]	Ref. [26]
frequency	2550 MHz	2480 MHz	2460 MHz	2540 MHz
Gain	−3.9 dBi	−8 dBi	0.47 dBi	Not given
BW	32 MHz	60 MHz	12 MHz	560 MHz
Total Size (mm)	$30 \times 30 \times 1.6$	$24 \times 24 \times 1.6$	$15 \times 15 \times 3.14$	$45 \times 14 \times 0.4$
Polarization	circular	linear	linear	linear

Table 4. Comparison for 3800 MHz.

parameter	First antenna	Ref. [27]	Ref. [28]	Ref. [9]
frequency	3850 MHz	3800 MHz	3660 MHz	3940 MHz
Gain	2.5 dBi	2.5 dBi	1.15 dBi	2.5 dBi
BW	100 MHz	260 MHz	620 MHz	139 MHz
Total Size (mm)	$30 \times 30 \times 1.6$	$40 \times 35 \times 1.6$	$20 \times 23.5 \times 1.6$	$76 \times 71 \times 1.6$
Polarization	linear	linear	Linear	circular

7. CONCLUSION

Periodic structures are investigated in antenna design for wireless applications, and these antennas have been compared with CRLH miniaturization method. Two novel compact and miniaturized antennas for wireless and GSM applications are presented in this article. The first antenna has directional pattern and is tri-band at 1760, 2550 and 3850 MHz with gains 2.1, −3.9 and 2.5 dBi, respectively, and it is dual polarized. The size of the prototype patch antenna is $20 \times 20\,\text{mm}^2$ in which the patch dimensions are reduced about 47% in comparison to conventional patch antenna at 2.5 GHz. The second antenna is designed by the use of interdigital capacitor and spiral inductor. Dimensions of the antenna are $15.5 \times 12\,\text{mm}^2$. So the size is reduced about 69% compared with conventional microstrip patch antennas at 1.8 GHz. The second antenna has three bands at 1060 MHz, 1800 MHz and 2500 MHz in which two frequencies (1.8 and 2.5 GHz) are suitable for GMS and WLAN applications. Both structures have been designed and fabricated on a FR4 low-cost substrate with $\varepsilon_r = 4.4$ and thickness of 1.6 mm.

ACKNOWLEDGMENT

The authors would like to thank Mr. Iraj Arghand and Mr. A. M. Shire for antenna testing. Their assistances are gratefully acknowledged.

REFERENCES

1. Song, X., "Small CPW-fed triple band microstrip monopole antenna for WLAN applications," *Microwave and Optical Technology Letters*, Vol. 51, No. 3, 747–749, 2009.
2. Ren, W., "Compact dual-band slot antenna for 2.4/5 GHz WLAN applications," *Progress In Electromagnetics Research B*, Vol. 8, 319–327, 2008.
3. Liu, J.-C., B.-H. Zeng, C.-Y. Liu, H.-C. Wu, and C.-C. Chang, "A dual-mode aperture-coupled stack antenna for WLAN dual-band and circular polarization applications," *Progress In Electromagnetics Research C*, Vol. 17, 193–202, 2010.
4. Ramli, N. H., M. R. Kamarudin, N. A. Samsuri, E. N. Ahyat, A. Y. Abdulrahman, and M. F. B. Jamlos, "A 6.0 GHz small printed monopole antenna for wireless implantable body area network (WiBAN) applications," *Progress In Electromagnetics Research C*, Vol. 41, 189–200, 2013.
5. Lee, B. and F. J. Harackiewicz, "Miniature microstrip antenna with a partially filled high-permittivity substrate," *IEEE Transactions on Antennas and Propagation*, Vol. 50, No. 8, 1160–1162, Aug. 2002.
6. Hu, Y., Y. J. Zhang, and J. Fan, "Equivalent circuit model of coaxial probes for patch antennas," *Progress In Electromagnetics Research B*, Vol. 38, 281–296, 2012.
7. Xiao, S., B.-Z. Wang, W. Shao, and Y. Zhang, "Bandwidth-enhancing ultralow-profile compact patch antenna," *IEEE Transactions on Antennas and Propagation*, Vol. 53, No. 11, 3443–3447, Nov. 2005.
8. Alam, M. S., M. T. Islam, and N. Misran, "A novel compact split ring slotted electromagnetic bandgap structure for microstrip patch antenna performance enhancement," *Progress In Electromagnetics Research*, Vol. 130, 389–409, 2012.
9. Yu, A., F. Yang, and A. Z. Elsherbeni, "A dual band circularly polarized ring antenna based on composite right and left handed metamaterial," *Progress In Electromagnetics Research*, Vol. 78, 73–81, 2008.
10. Sayem, A. T. M. and M. Ali, "Characteristics of a microstrip-fed miniature printed Hilbert slot antenna," *Progress In Electromagnetics Research*, Vol. 56, 1–18, 2006.
11. Li, M., H.-L. Yang, X.-W. Hou, Y. Tian, and D.-Y. Hou, "Perfect metamaterial absorber with dual bands," *Progress In Electromagnetics Research*, Vol. 108, 37–49, 2010.
12. Buell, K., H. Mosallaei, and K. Sarabandi, "A substrate for small patch antennas providing tunable miniaturization factors," *IEEE Transactions on Microwave Theory and Techniques*, Vol. 54, No. 1, 135–146, 2006.
13. Bilotti, F., A. Alú, and L. Vegni, "Design of miniaturized metamaterial patch antennas with μ-negative loading," *IEEE Transactions on Antennas and Propagation*, Vol. 56, No. 6, 1640–1647, 2008.
14. Gurel, L., A. Unal, and T. Malas, "Fast and accurate analysis of large metamaterial structures using the multilevel fast multipole algorithm," *Progress In Electromagnetics Research*, Vol. 95, 179–198, 2009.
15. Majid, H. A., M. K. Abd Rahim, and T. Masri, "Microstrip antenna's gain enhancement using left-handed metamaterial structure," *Progress In Electromagnetics Research M*, Vol. 8, 235–247, 2009.
16. Zhao, L., D. Yang, H. Tian, Y. Ji, and K. Xu, "A pole and AMC point matching method for the synthesis of HSF-UC-EBG structure with simultaneous AMC and EBG properties," *Progress In Electromagnetics Research*, Vol. 133, 137–157, 2013.

17. Ouedraogo, R. O., E. J. Rothwell, A. R. Diaz, K. Fuchi, and A. Temme, "Miniaturization of patch antennas using a metamaterial-inspired technique," *IEEE Transactions on Antennas and Propagation*, Vol. 60, No. 5, 2175–2182, 2012.
18. Antoniades, M. A. and G. V. Eleftheriades, "A broadband dual-mode monopole antenna using NRI-TL metamaterial loading," *IEEE Antennas and Wireless Propagation Letters*, Vol. 8, 258–261, 2009.
19. Niu, J.-X., "Dual-band dual-mode patch antenna based on resonant-type metamaterial transmission line," *Electronics Letters*, Vol. 46, No. 4, 266–268, 2010.
20. Zhu, J. and G. V. Eleftheriades, "A compact transmission-line metamaterial antenna with extended bandwidth," *IEEE Antennas and Wireless Propagation Letters*, Vol. 8, 295–298, 2009.
21. Azimi Fashi, A., M. Kamyab, and M. Barati, "A microstrip small-sized array antenna based on the meta-material zeroth-order resonator," *Progress In Electromagnetics Research C*, Vol. 14, 89–101, 2010.
22. Rafael Booket, M., M. Veysi, Z. Atlasbaf, and A. Jafargholi, "Ungrounded composite right-/left-handed metamaterials design, synthesis and applications," *IET Microwaves, Antennas and Propagation*, Vol. 6, No. 11, 1259–1268, 2012.
23. Park, J.-H., Y.-H. Ryu, J.-G. Lee, and J.-H. Lee, "Epsilon negative zeroth-order resonator antenna," *IEEE Transactions on Antennas and Propagation*, Vol. 55, No. 12, 3710–3712, 2007.
24. Segovia-Vargas, D., F. J. Herraiz-Martinez, E. Ugarte-Munoz, L. E. Garcia-Munoz, and V. Gonzalez-Posadas, "Quad-frequency linearly-polarized and dual-frequency circularly-polarized microstrip patch antennas with CRLH loading," *Progress In Electromagnetics Research*, Vol. 133, 91–115, 2013.
25. Oh, J. and K. Sarabandi, "Low profile, miniaturized, inductively coupled capacitively loaded monopole antenna," *IEEE Transactions on Antennas and Propagation*, Vol. 60, No. 3, 1206–1213, 2012.
26. Selvanayagam, M. and G. V. Eleftheriades, "A compact printed antenna with an embedded double-tuned metamaterial matching network," *IEEE Transactions on Antennas and Propagation*, Vol. 58, No. 7, 2354–2361, 2010.
27. Ha, J., K. Kwon, Y. Lee, and J. Choi, "Hybrid mode wideband patch antenna loaded with a planar metamaterial unit cell," *IEEE Transactions on Antennas and Propagation*, Vol. 60, No. 2, 1143–1147, 2012.
28. Zhu, J., M. A. Antoniades, and G. V. Eleftheriades, "A compact tri-band monopole antenna with single-cell metamaterial loading," *IEEE Transactions on Antennas and Propagation*, Vol. 58, No. 4, 1031–1038, 2010.